Postprint of: Skibicki J., The issue of uncertainty of visual measurement techniques for long distance measurements based on the example of applying electric traction elements in diagnostics and monitoring, MEASUREMENT, Vol. 113 (2018), pp. 10-21, DOI: 10.1016/j.measurement.2017.08.033

The issue of uncertainty of visual measurement techniques for long distance measurements based on the example of applying electric traction elements in diagnostics and monitoring.

Abstract

Rail transport is the most economical and energy-effective in the field of land transport, in particular electrified. In order to ensure efficient and reliable operation of electrified rail transport, the issues of monitoring and diagnostics of the traction infrastructure and vehicles are extremely important. The most critical point in the transmission of electric energy to the vehicle is the sliding contact of the current collector with the traction network. For this reason, work is currently being carried out on the possibility of monitoring the technical condition of current collectors at selected points of the railway lines, which makes it possible to detect the current collectors which do not work properly, and those in which the damage occurred after the train's departure. In order to make the diagnostic process at such point as complete as possible, it is necessary to develop new measurement methods and new applications for the existing methods. Evaluation of the technical condition of current collectors at the control point is carried out based on the analysis of displacements of the contact wire of the overhead contact line, caused by the impact of the current collector. The nature of these displacements, as well as the presence or absence of certain components provides the information on the correct adjustment of the current collector and the technical condition of its strips. Simultaneous measurement of vertical and horizontal displacements requires the application of innovative measurement techniques. The use of non-contact visual techniques for this purpose, which makes it possible to measure displacements in a two-dimensional plane using a fast 2D camera and advanced image analysis, is promising. This article presents the analysis of measurement uncertainty of visual measurement techniques for long distance measurements for application of electric traction element diagnostic and monitoring. The measurement verification at a laboratory test stand are also presented. The requirements concerning the measurement equipment have been determined and the factors affecting the uncertainty of the final measurement dependent on a given configuration of the stand have been specified.

1. Introduction

The increasing mobility of modern societies, as well as liberalization of the economic market are causing an increased demand for passenger and freight transport. Rail transport is the most economical and energy-effective in the field of land transport, in particular electrified. In order to ensure efficient and reliable operation of electrified rail transport, the issues of monitoring and diagnostics of the traction infrastructure and vehicles are extremely important. The most critical point in the transmission of electric energy to the vehicle is the sliding contact of the current collector with the traction network. Even a minor defect of any part of this contact (such as chipping of the shoe's contact strip) can often lead to severe damage of the infrastructure and/or vehicle, resulting in significant financial losses, as well as causing perturbations and disruptions in railway traffic. For this reason, work is currently being carried out on the possibility of monitoring the technical condition of current collectors at selected points of the railway lines, which makes it possible to detect the current collectors which do not work properly, and those in which the damage occurred after the train's departure. In order to make the diagnostic process at such point as complete as possible, it is necessary to develop new measurement methods and new applications for the existing methods. The principle here is that the measuring equipment should not interfere with the traction network parameters, or that such interference should be as small as possible.

Evaluation of the technical condition of current collectors at the control point is carried out based on the analysis of displacements of the contact wire of the overhead contact line, caused by the impact of the current collector. The nature of these displacements, as well as the presence or absence of certain components provides the information on the correct adjustment of the current collector and the technical condition of its strips. For example, too low or too high vertical displacement of the wire indicates the incorrect adjustment of pressure, and the presence of horizontal displacements may indicate chipping or pitting in the shoe strip. Only vertical displacement measurements with the use of a short-range laser rangefinder, or other measurement techniques are performed at the currently functioning stands [1, 2], which limits the functionality of such stands.

Simultaneous measurement of vertical and horizontal displacements requires the application of different measurement techniques. The use of non-contact visual techniques for this purpose, which makes it possible to measure displacements in a two-dimensional plane using a fast 2D camera and advanced image analysis, is promising [3]. Visual measurement techniques in traction applications have so far been applied in measuring the geometry of overhead contact lines[4–12], as well as in measuring the wear of the contact wire [4, 13, 14]. The evaluation of the technical condition of strips is carried out with the use of 3D laser scanning systems [15–18]. Therefore, the proposed use of a 2D camera and determination of the technical condition of the current collector based on the analysis of displacements of the contact wire is an innovative application of visual measurement techniques. Thanks to the proposed visual technique it is possible to measure the displacements not only of single contact wire, but also of the catenary wire. In the case of contact lines consisting of two contact wires, or other more complex configurations, displacements of each contact wire or catenary wire can be measured independently without any hardware upgrades. This is a great advantage of the proposed method, compared to the existing solutions, where each increase in the number of measurement elements required a corresponding increase in the number of sensors. In addition, the possibility of complex monitoring of the response of the contact line to the influence of the current collector will allow for a more accurate analysis of the correctness of cooperation of these elements.

Prior to carrying out measurements, it is necessary to perform an analysis of measurement uncertainty for such a stand, so as to determine whether the accuracy obtained is going to meet the requirements of the measurement object.

This article presents the above-mentioned analysis along with the measurement verification at a laboratory test stand. The requirements concerning the measurement equipment have been determined and the factors affecting the uncertainty of the final measurement dependent on a given configuration of the stand have been specified.

2. Object of measurement

The object of the measurement is to register the displacement of the contact wire of the overhead contact line in a two-dimensional plane, caused by the impact of the current collector of a passing traction vehicle. With regard to controlling the correctness of the current collector contact force regulation, and to monitoring the technical condition of its strips, the measurement point should be located half way along the suspension span. This is due to the fact that the degree of flexibility of the contact line is the highest at this point, and therefore the influence of the current collector will be the strongest there. Naturally, for such a configuration, the displacements measured at this point will be smaller when the current collector is at the end of the span than when it reaches its middle. However, the damage of the strip should always result in a measurable displacement in the horizontal axis. Such a displacement may be regarded as a signal that the damage has been detected. Values of these

displacements do not normally exceed +/-10 cm, both in the vertical axis and in the horizontal axis in relation to the resting position. Since the contact wire is located at the height of about 5.5 m above the railhead, and because it is necessary to remain at a certain distance due to vehicle gauge, terrain configuration at the measurement site or other factors which prevent a close approach to the measured object, the distance from which the measurements are to be performed can be about a dozen or even a few dozen metres. This distance can therefore be several hundred times greater than the measured displacement values. Such measurements can, therefore, be classified as long distance measurements. Such an approach in monitoring and diagnostics of current collectors and overhead contact lines is new, since in the solutions available so far, the distances from which visual contact-less measurements are performed do not normally exceed a few metres [9, 10, 12, 19].

3. Measurement stand – configuration and requirements

To register the displacements of the contact wire of the overhead contact line in a two-dimension plane using a 2D camera, a measurement stand with the configuration shown in Fig.1 can be used.

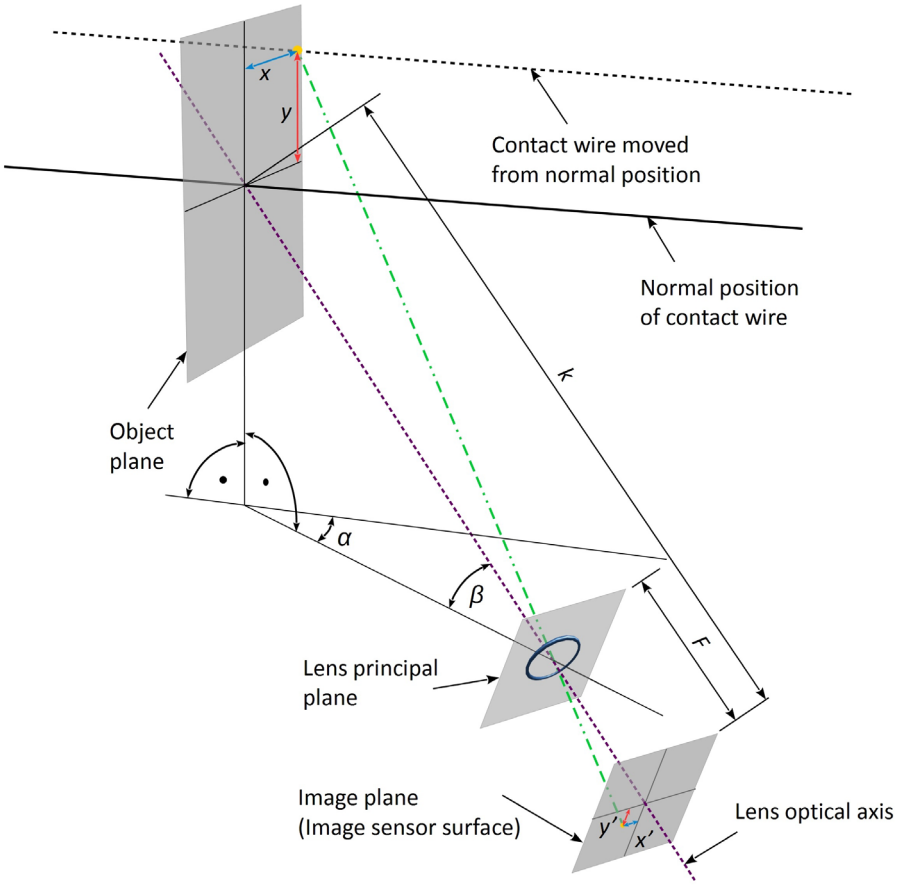

Fig. 1. Configuration of the measurement stand for testing the contact wire displacements of the overhead contact line in two axes using a 2D imaging camera, where: x, y – displacement of the contact wire in the horizontal and vertical axis respectively; x', y' – displacement of the image on the camera matrix in the horizontal and vertical axis respectively, k – distance between the central point of the object plane and the image plane, F – distance between the main plane of the lens and the camera matrix (plane of the image); α – angle between the vertical plane in which the contact wire lies and the vertical plane in which the optical axis of

the lens lies; β – angle of inclination of the optical axis of the lens in relation to the horizontal one.

For the configuration of the measuring system shown in Fig. 1, the dependence showing the displacement of the object in the horizontal axis based on the analysis of the position of its image on the surface of the matrix is given by the following formula:

$$x = \frac{(k-F)\cdot x\prime\cdot\cos\beta}{\cos\alpha\cdot(F\cdot\cos\beta - y'\cdot\sin\beta) - x\prime\cdot\sin\alpha} \quad (1)$$

An analogous dependence for the vertical axis is as follows:

$$y = \frac{(k-F)\cdot(y' + x\prime\cdot sin\beta\cdot tan\alpha)}{F\cdot cos\beta - y\prime\cdot sin\beta - x\prime\cdot tan\alpha} \quad (2)$$

The distance F between the optical centre of the lens and the imaging plane depends on the focal length of the lens and the reproduction ratio and is given by:

$$F = \frac{k-\sqrt{k^2-4\cdot k\cdot f}}{2} \quad (3)$$

where: f – focal length of the lens.

In contrast, the focal length of the lens depends on the current distance setting and is given by the following formula:

$$f = \frac{k}{2+\frac{x\prime}{x}+\frac{x}{x\prime}} \quad (4)$$

where: x' - image size of the object with x dimensions.

An uncertainty analysis was carried out assuming a constant angle value $\alpha = 45^{o}$ being maintained and the change of all the other values, with these changes being closely interlinked. Assuming that the measurements are made on a flat terrain and the camera is mounted at a constant height above the ground, then when increasing the distance k from the measured object, the pitch of the camera, i.e. the angle β, will decrease and, in order to maintain the reproduction ratio, it will be necessary to simultaneously increase the focal length of the lens f. Basler acA 2040-180kc camera with the following basic technical specification was used as a measurement camera:

- matrix resolution: 2046x2046 px (4 mpix);
- matrix size: 11.26x11.26 mm;
- maximum recording speed: 180 fps.

3.1. Minimum measurement distance

For the assumed value of the angle α there is a minimum distance k_{min} for which measurements can be performed. It results from the vehicle gauge as well as the catenary construction zone and current collector zone. It has been shown in Fig. 2.

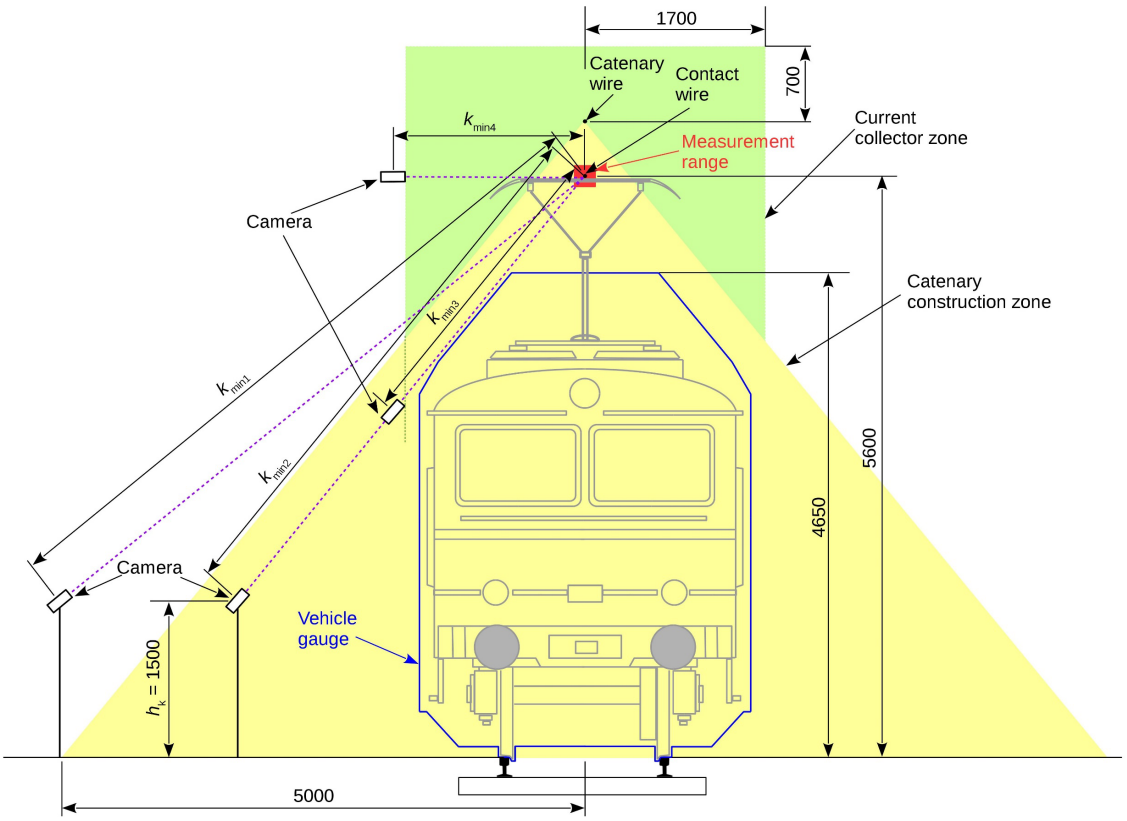

Fig. 2. Method for determining minimum value k_{min}

For the situation shown in Fig. 2. four values k_{min} have been marked. They are related to the constraints resulting from the individual zones located near the railway line. The value k_{min1} results from the limitations caused by the catenary construction. The catenary construction zone is an equilateral triangle-shaped area, with its tip in the catenary axis and its arms extending to the distance of 5 m from the track axis on both sides, measured at the railhead height. Placing the camera outside this zone allows complete freedom with regard to its mounting and power supply. There are also no other limitations. Distances k_{min2} and k_{min3} lie inside this zone, which translates into the necessity of bonding or grounding all elements located in it (camera case, mounting structure, etc.). In addition, the distance k_{min2} results from the limitation associated with the vehicle gauge. This limitation is associated with the fact that the passing vehicle cannot obscure the contact wire seen by the camera. When the camera is moved closer, to the distance k_{min3}, the current collector zone is reached. This zone is an area in the immediate vicinity of the catenary construction, reaching up to 70 cm above the catenary and extending 1.7 m in each direction, measured from the track axis. It is practically impossible and not recommended for safety reasons to place such objects as cameras within this area. Therefore, in order to further reduce the distance k, it is necessary to move along the border of the current collector zone until the absolute minimum for the value k_{min4} is reached. At this distance, angle β takes zero value. Further reduction of the distance k, assuming a constant value of angle α, is not possible. It is recommended, however, to keep the camera "looking" up (angle $\beta > 0^{o}$), since the analysis of the image placed against a uniform background of the sky is much less complicated compared with the image whose background consists of contrasting elements with numerous details.
Assuming that in the situation where $k \geq k_{min2}$, the camera will be mounted at the height h_k = 1.5 m above the railhead, as well as taking into account that the angle α has a constant invariable value of 45º, the minimum distances k will amount to, respectively: k_{min1} = 8.2 m,

k_{min2} = 6.2 m, k_{min3} = 3.2 m and k_{min4} = 2.4 m. Along with the decrease of the distance k, the value of angle β will change as follows:

$$\beta = \begin{cases} \arcsin\left(\frac{h-h_k}{k}\right) & \text{for} \quad k \geq k_{min2} \\ \arcsin\left(\frac{h-h_k}{k_{min2}}\right) & \text{for} \quad k_{min3} \leq k < k_{min2} \\ \arccos\left(\frac{k_{min4}}{k}\right) & \text{for} \quad k_{min4} \leq k < k_{min3} \end{cases} \quad (5)$$

3.2. Maximum measurement distance

It may often be necessary to increase the distance k. This may, for example, be the case when another track or tracks are located between the track on which the test is being carried out and the place where the camera is mounted. The increase the distance has limits related to the maximum focal length of the lens f which can be used. The required focal length of the camera lens can be calculated from the dependence (4).
For the case in question, with the assumed vertical and horizontal displacements measurement range ±100 mm, the permissible excess of the range equal 20%, and for the proposed camera type, the dependence between the minimum focal length of the lens and the required distance k is shown in Fig. 3.

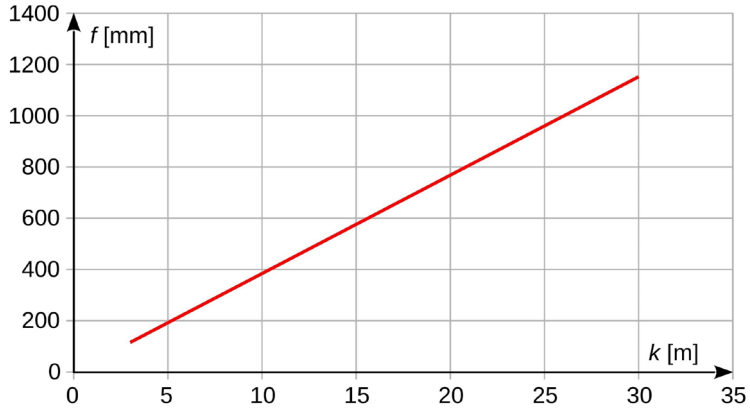

Fig. 3. Dependence between the focal length of the lens f and the matrix distance of the matrix from the measured object k

As the calculations, whose results are presented in Fig. 3, show, it is necessary to use lenses with long or very long focal length at the measuring stand. The measurement object requires lenses with the lowest possible level of distortion, which practically excludes the use of variable focus lenses. Unfortunately, typical fixed-focus lenses with C-mount used for industrial cameras which would have such long focal lengths are not produced (the maximum focal length of typical C-mount lenses is f = 100 mm). The only solution is to use lenses designed for 35mm film cameras and mount them with a suitable adapter. Focal lengths of currently manufactured lenses for 35mm SLR cameras reach up to f = 800 mm. Previously, lenses with longer focal lengths, namely f = 1000, 1200, 1600, and even 2000 mm, were manufactured. It is therefore possible to select an appropriate focal length of the lens for given requirements. Restricting ourselves to more easily accessible lenses (with regard to price and supply), the focal length f = 1000 mm limit will be the limit here, which determines, for the stand configuration in question, the maximum measurement distance as k_{max} = 26 m.

4. Analysis of measurement uncertainties

4.1. Sensitivity coefficients

In line with dependencies (1) and (2), the results of displacement measurements s in both axes depend on six values, i.e. standard measurement uncertainties will depend on the uncertainty of measurement of all intermediate values. Therefore, it can be write as follows:

$$u(x) = \mathrm{f}\big(u(k); u(F); u(x'); u(y'); u(\alpha); u(\beta)\big) \quad (6)$$

and:

$$u(y) = \mathrm{f}\big(u(k); u(F); u(x'); u(y'); u(\alpha); u(\beta)\big) \quad (7)$$

The impact of individual uncertainty of partial measurements on the uncertainty of the final measurement depends on the value of the so-called sensitivity coefficient for the given value. For horizontal displacement measurements, the sensitivity coefficients are:

- the measurement of distance *k*:

$$\frac{\partial x}{\partial k} = \frac{x\prime \cdot cos\beta}{cos\alpha \cdot (F \cdot cos\beta - y' \cdot sin\beta) - x\prime \cdot sin\alpha} \quad (8)$$

- the measurement of *F* distance:

$$\frac{\partial x}{\partial F} = \frac{x\prime \cdot cos\beta \cdot [cos\alpha \cdot (y' \cdot sin\beta - k \cdot cos\beta) + x\prime \cdot sin\alpha]}{[cos\alpha \cdot (F \cdot cos\beta - y' \cdot sin\beta) - x\prime \cdot sin\alpha]^2} \quad (9)$$

- the measurement of the position of a point on the matrix surface in the horizontal axis x':

$$\frac{\partial x}{\partial x\prime} = \frac{(k-F) \cdot cos\beta \cdot cos\alpha \cdot (F \cdot cos\beta - y\prime \cdot sin\beta)}{[cos\alpha \cdot (F \cdot cos\beta - y' \cdot sin\beta) - x\prime \cdot sin\alpha]^2} \quad (10)$$

- the measurement of the position of a point on the matrix surface in the vertical axis y':

$$\frac{\partial x}{\partial y\prime} = \frac{0.5 \cdot (k-F) \cdot x\prime \cdot cos\alpha \cdot sin2\beta}{[cos\alpha \cdot (F \cdot cos\beta - y' \cdot sin\beta) - x\prime \cdot sin\alpha]^2} \quad (11)$$

- the measurement of α angle:

$$\frac{\partial x}{\partial \alpha} = \frac{(k-F) \cdot x\prime \cdot cos\beta \cdot [sin\alpha \cdot (F \cdot cos\beta - y' \cdot sin\beta) + x\prime \cdot cos\alpha]}{[cos\alpha \cdot (F \cdot cos\beta - y' \cdot sin\beta) - x\prime \cdot sin\alpha]^2} \quad (12)$$

- the measurement of β angle:

$$\frac{\partial x}{\partial \beta} = \frac{(k-F) \cdot x\prime \cdot (y\prime \cdot cos\alpha + x\prime \cdot sin\alpha \cdot sin\beta)}{[cos\alpha \cdot (F \cdot cos\beta - y' \cdot sin\beta) - x\prime \cdot sin\alpha]^2} \quad (13)$$

Similarly, for measurements of displacements in a vertical axis we obtain:

- the measurement of distance *k*:

$$\frac{\partial y}{\partial k} = \frac{y' + x\prime \cdot sin\beta \cdot tan\alpha}{F \cdot cos\beta - y\prime \cdot sin\beta - x\prime \cdot tan\alpha} \quad (14)$$

- the measurement of F distance:

$$\frac{\partial y}{\partial F} = \frac{(y' + x\prime \cdot sin\beta \cdot tan\alpha) \cdot (y\prime \cdot sin\beta + x\prime \cdot tan\alpha - k \cdot cos\beta)}{(F \cdot cos\beta - y\prime \cdot sin\beta - x\prime \cdot tan\alpha)^2} \quad (15)$$

- the measurement of the position of a point on the matrix surface in the horizontal axis x':

$$\frac{\partial y}{\partial x\prime} = \frac{(k-F) \cdot tan\alpha \cdot cos\beta \cdot (F \cdot sin\beta + y\prime \cdot cos\beta)}{(F \cdot cos\beta - y\prime \cdot sin\beta - x\prime \cdot tan\alpha)^2} \quad (16)$$

- the measurement of the position of a point on the matrix surface in the vertical axis y':

$$\frac{\partial y}{\partial y\prime} = \frac{(k-F) \cdot cos\beta \cdot (F - x\prime \cdot cos\beta \cdot tan\alpha)}{(F \cdot cos\beta - y\prime \cdot sin\beta - x\prime \cdot tan\alpha)^2} \quad (17)$$

- the measurement of α angle:

$$\frac{\partial y}{\partial \alpha} = \frac{(k-F) \cdot x\prime \cdot cos\beta \cdot sec^2\alpha \cdot (F \cdot sin\beta + y\prime \cdot cos\beta)}{(F \cdot cos\beta - y\prime \cdot sin\beta - x\prime \cdot tan\alpha)^2} \quad (18)$$

- measurement of the β angle:

$$\frac{\partial y}{\partial \beta} = \frac{(k-F) \cdot [x\prime \cdot tan\alpha \cdot (F - cos\beta \cdot tan\alpha) + y\prime \cdot (y\prime \cdot cos\beta + F \cdot sin\beta)]}{(F \cdot cos\beta - y\prime \cdot sin\beta - x\prime \cdot tan\alpha)^2} \quad (19)$$

Dependencies between the values of sensitivity coefficients and distance of the camera from the object, for the measurements in horizontal axis are shown in Fig. 4. The results are presented for the parameters of the stand shown in 3.1 and 3.2.

a)

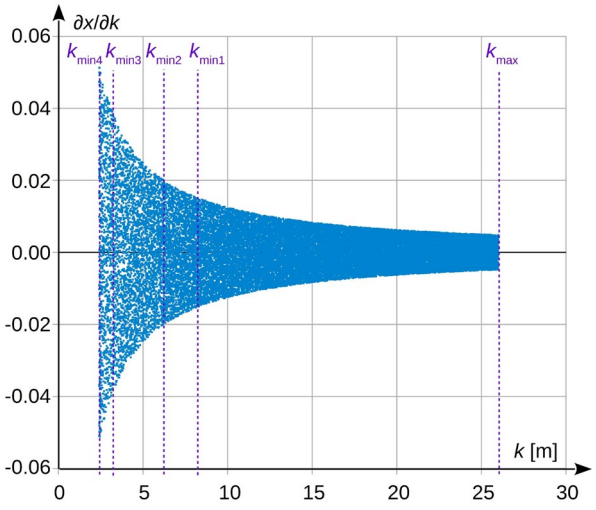

b)

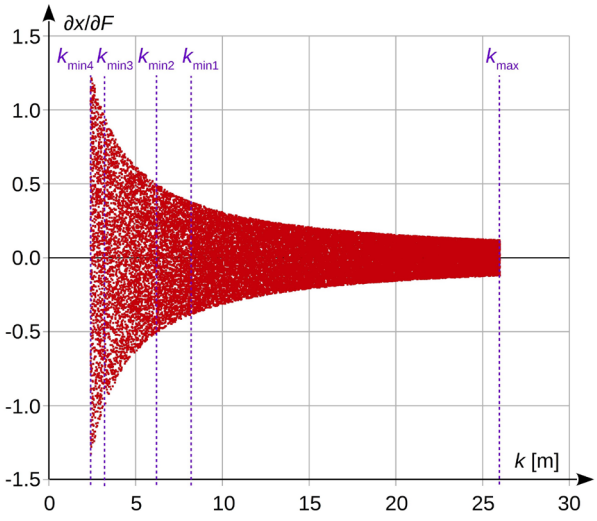

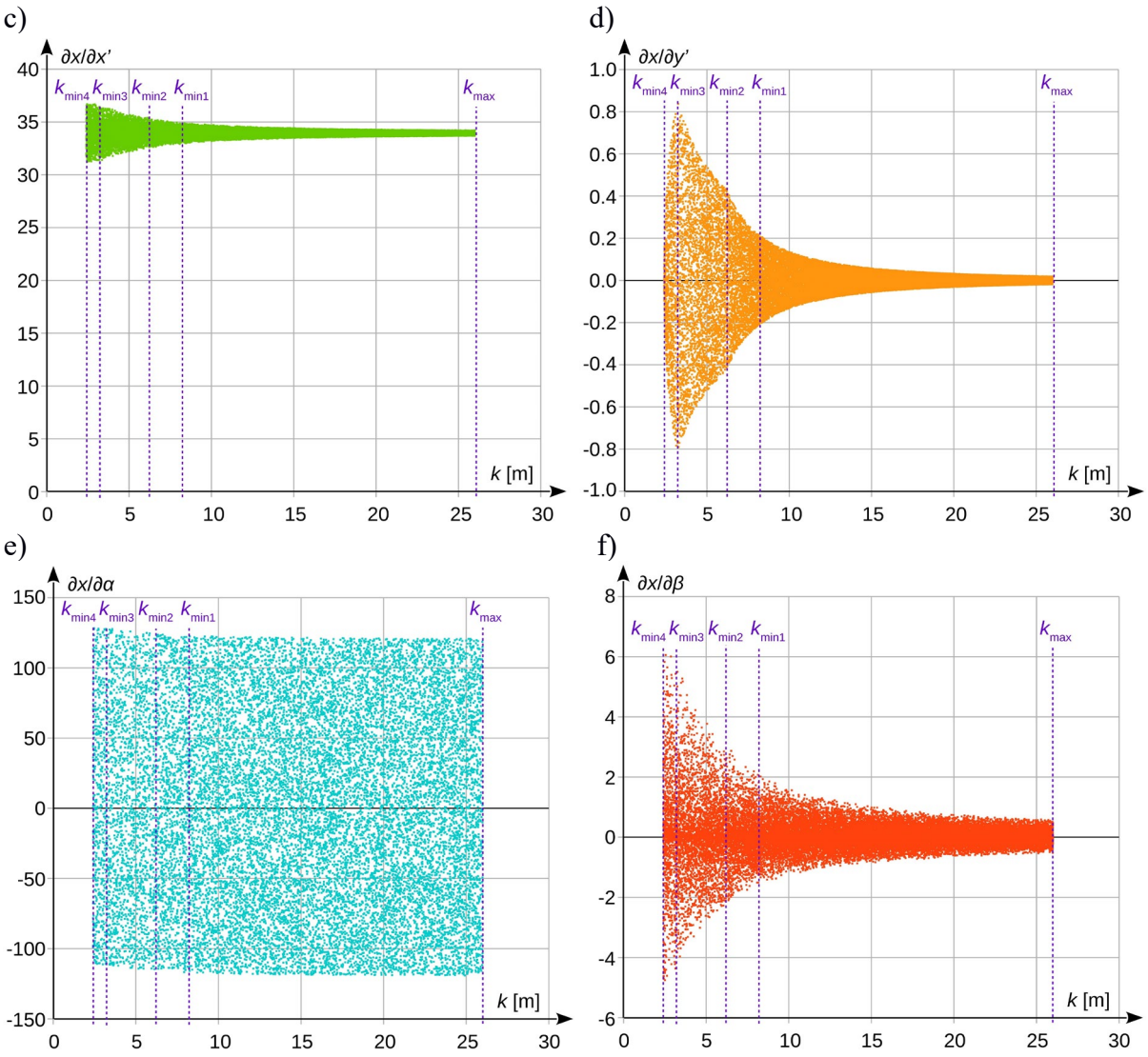

Fig. 4. Sensitivity coefficients for measurements in the horizontal axis as a function of distance k, where: a) measurement of distance k; b) measurement of distance F; c) measurement of the position of the point on the matrix surface in the horizontal axis x'; d) measurement of the position of the point on the matrix surface in the vertical axis y'; e) measurement of angle α; f) measurement of angle β.

Similarly, the values of the coefficients for measurement in the vertical axis are shown in Fig. 5.

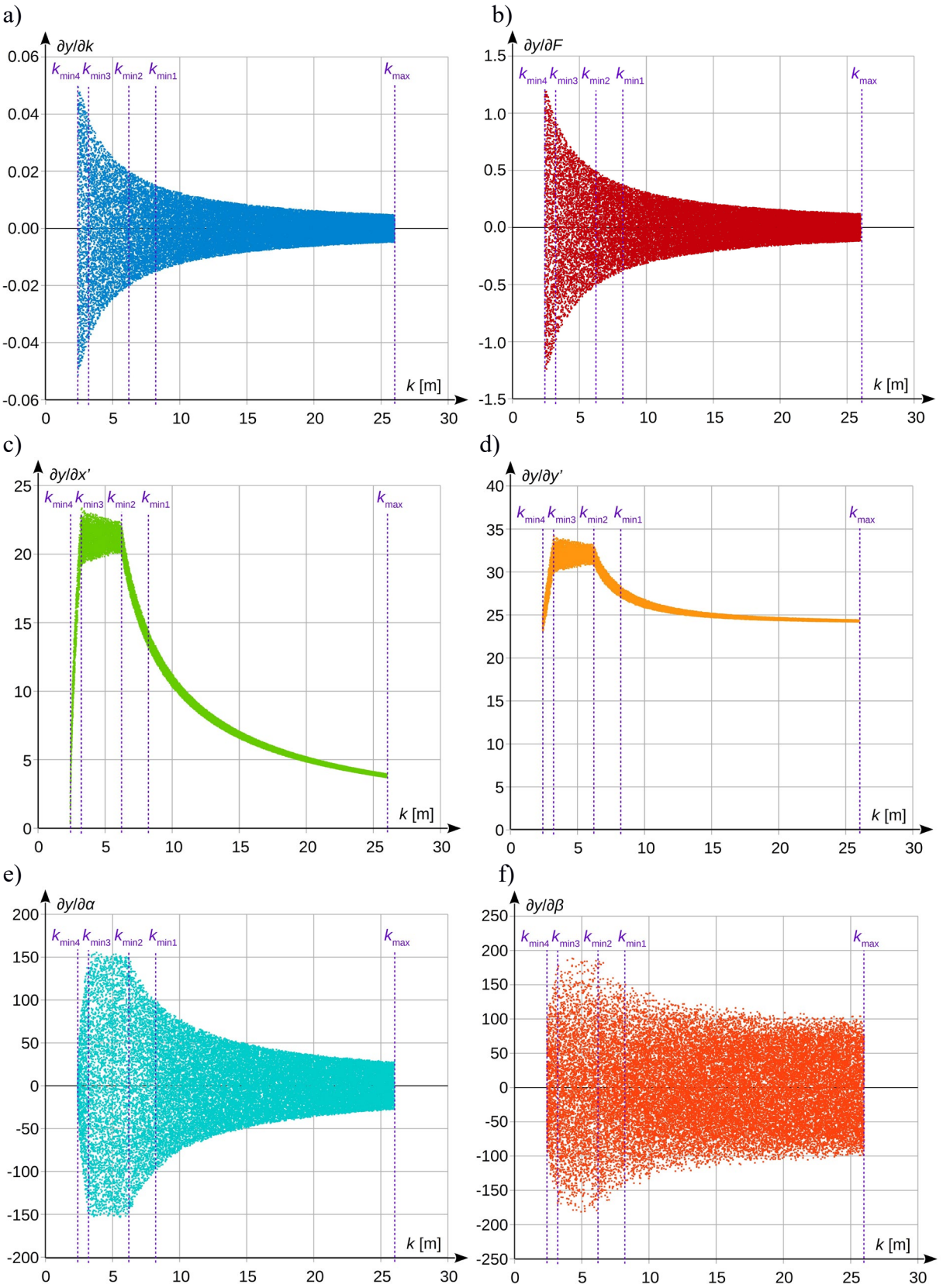

Fig. 5. Sensitivity coefficients for measurements in vertical axis as a function of the distance k, where: a) measurement of distance k; b) measurement of distance F; c) measurement of the position of the point on the matrix surface in the horizontal axis x'; d) measurement of the position of the point on the matrix surface in the vertical axis y'; e) measurement of angle α; f) measurement of angle β.

The analysis of sensitivity coefficients shows that for the discussed case the values of these factors considerably decrease as the distance k increases, and only for some of them there is an initial increase in the values of distance k for the range between k_{min4} and k_{min3}; then a relatively constant value is maintained when the distance k falls within the range between k_{min3} and k_{min2}, and only the increase of the distance above k_{min2} causes a decrease in the value of the coefficient. These relationships are caused by changes in the value of angle β and their impact on the values of the said coefficients.

4.2. Selection of measuring instruments

Since the discussed measurements fall within the scope of technical engineering measurements, it is assumed, for the purpose of the measurement uncertainty analysis, that typical measuring instruments for laboratory use will be used. The equipment used in measurements has been listed in Table 1.

Table 1. The list of measurement equipment used, together with its purpose

No.	Name	Calibration uncertainty	Purpose
1.	Basler acA 2040-180 kc camera with a full set of lenses with different focal lengths	Depends on the distance k	Measurement of the object's image position on the matrix x' and y'; Indirect measurement of distance F
2.	Professional laser rangefinder BOSCH GLM 80	±1.5 mm	The measurement of distance k; Indirect measurement of angle α; Indirect measurement of distance F
3.	FWP MADb 400 calliper	±0.05 mm	Indirect measurement of distance F
4.	ACS-080-2-SC00-HE2-2W inclinometer	±0.1º	The measurement of angle β; Indirect measurement of angle α

4.3. Analysis of measurement uncertainties in indirect measurements

4.3.1. Measurement of distance k

The measurement of distance k is a direct measurement carried out with the use of a professional laser rangefinder Bosch GLM 80. The manufacturer declares that, under normal measurement conditions, the calibration uncertainty is constant within the entire measuring range and amounts to $\Delta k = \pm 1.5$ mm. Thus, the value of the standard uncertainty necessary to determine the uncertainty of other indirect measurements will also be independent of the distance k and amount to:

$$u(k) = \frac{\Delta k}{\sqrt{3}} = \frac{1.5}{\sqrt{3}} = 0.87 \text{ mm} \quad (20)$$

4.3.2. Measurement of distance F

The measurement of distance F is an indirect measurement carried out based on the dependence (3). After substituting dependence (4) with dependence (3) and simplification we obtain:

$$F = \frac{k}{2} \cdot \left(1 - \sqrt{1 - \frac{4 \cdot x_w \cdot x'_w}{(x_w + x'_w)^2}}\right) \quad (21)$$

where: x_w – the size of the model with known dimensions; x'_w – the size of the model image on the camera matrix

Since the reproduction ratio does not change (values x_w and x'_w are constant), the distance F depends on the current distance k. Therefore, the standard uncertainty of measurement of distance F depends on the uncertainty of measurement of distance k as well as value x and x', and is given by the following dependence:

$$u(F) = \sqrt{\left(\frac{\partial F}{\partial k}\right)^2 \cdot u(k)^2 + \left(\frac{\partial F}{\partial x_w}\right)^2 \cdot u(x_w)^2 + \left(\frac{\partial F}{\partial x'_w}\right)^2 \cdot u(x'_w)^2} \quad (22)$$

Standard uncertainty of the measurement of distance k is provided in (20). The measurements of values x_w and x'_w, i.e. dimensions of the object and the image thereof are direct measurements. The value x_w is measured with the use of FWP MADb 400 calliper, with calibration uncertainty $\Delta x_w = \pm 0.05$ mm. Therefore, the standard uncertainty in the measurement of this value is given by relationship analogous to (20) and amounts to:

$$u(x_w) = \frac{\Delta x_w}{\sqrt{3}} = \frac{0.05}{\sqrt{3}} = 0.029 \text{ mm} \quad (23)$$

The value of x'_w is determined based on the observation of the image obtained from the camera. It can be determined with the uncertainty of the experimenter at the level of one pixel, i.e. $\Delta x'_{we} = \pm 0.0055$ mm. Since the manufacturer does not define uncertainty for the determination of the dimensions of a single pixel, and indicates only the total size of the matrix, i.e.11.26x11.26 mm, the standard uncertainty of a single pixel was established on assumption that the matrix size had been determined with the uncertainty at the level of the last significant figure in the result, namely ±0.01 mm. In such system, taking into account the matrix resolution of 2046x2046 pixels, the standard uncertainty of the size of a single pixel amounts to ±0.0029 μm, which means that it can be disregarded, since it is smaller by three orders of magnitude from the assumed experimenter's uncertainty. Therefore, the standard uncertainty of measurement of value x' will be equal to:

$$u(x') = \frac{\Delta x'_{we}}{\sqrt{3}} = \frac{0.0055}{\sqrt{3}} = 0.0032 \text{ mm} \quad (24)$$

Having taken into account the uncertainty of partial measurements, the standard uncertainty of the measurement of value F related to the distance k for the case in question is shown in Fig. 6.

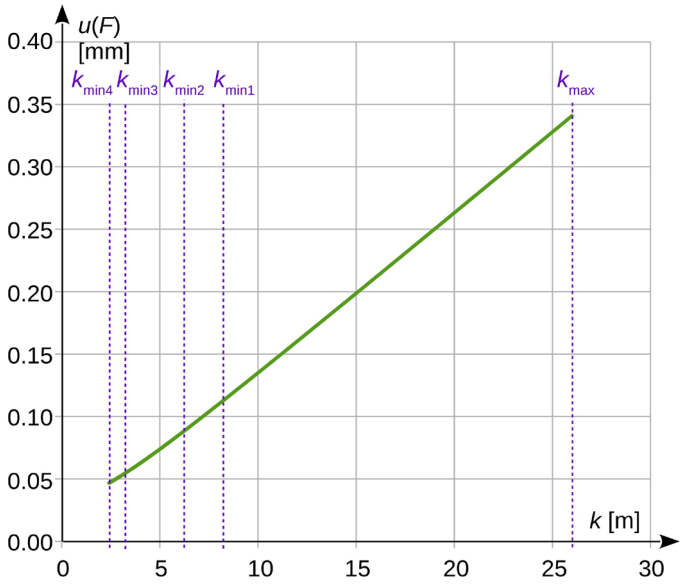

Fig. 6. Standard uncertainty $u(F)$ as a function of distance k

4.3.3. The measurement of angle β

The measurement of angle β is performed directly with the use of ACS-080-2-SC00-HE2-2W inclinometer. The manufacturer defines the level of calibration uncertainty as $\Delta\beta = \pm 0.1^{\circ}$. Taking into account the indirect way of reading the result (measurement of the voltage applied to the calibration resistor connected to the inclinometer current output), standard uncertainty of the measurement of angle β amounts to $u(\beta) = 0.067^{\circ}$ and is independent of the current distance k value.

4.3.4. Measurement of angle α

In the discussed case, due to the long distance between the camera and the measured object, the direct measurement of angle α is impossible. The only option is to perform indirect measurement based on trigonometric dependencies, as shown in Fig. 7a.

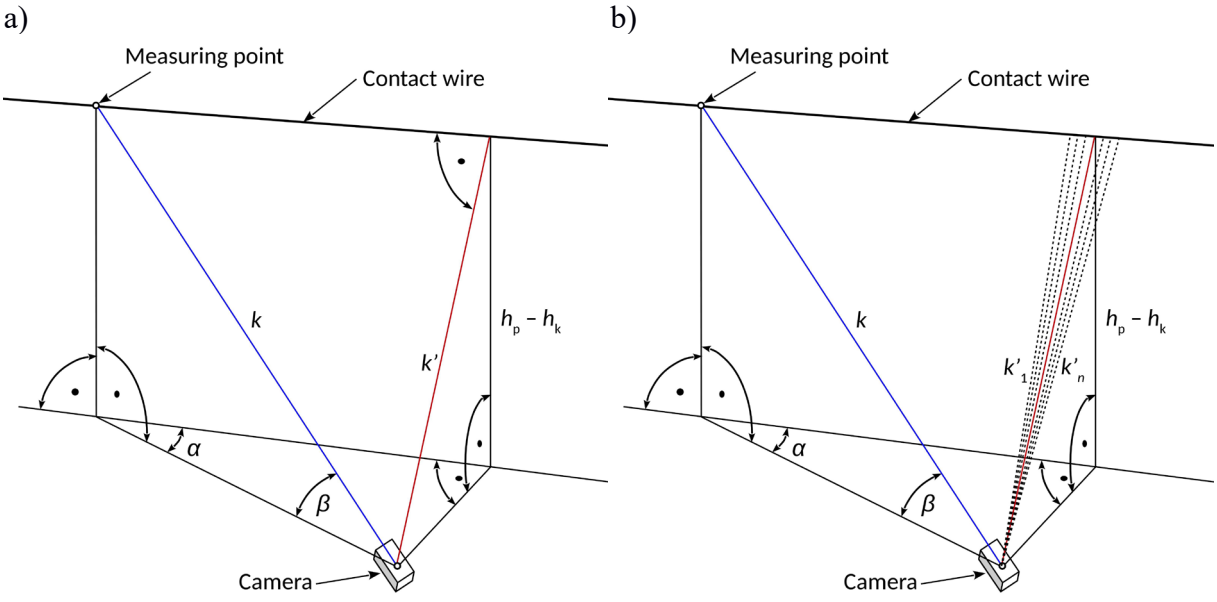

Fig. 7. Indirect measurement of angle α, where: a) spatial layout; b) determination of value k'

Taking into account the measurable values k, k' and β, the value of angle α is given by the dependence:

$$\alpha = \arcsin\left(\frac{\sqrt{k'^2-(k\cdot\sin\beta)^2}}{k\cdot\cos\beta}\right) (25)$$

A certain problem, particularly when distance k is a dozen or more metres, is the measurement of distance k' performed in such a way that it is measured at a right angle to the contact wire. The solution here is to perform a series of measurements with a slightly changed angular position of the laser rangefinder, as shown in Fig. 7b. The sought value k' will then be the smallest result obtained, which is:

$$k' = \min(k'_i)|_{i=1}^{n} \quad (26)$$

The uncertainty in measurements of distances k and k' stems from the uncertainty of the laser rangefinder calibration and is constant, regardless of the measurement distance, as discussed in p. 4.3.1. The uncertainty in measurement of angle β is also a constant value, and depends on the inclinometer calibration uncertainty (see p. 4.3.3.). Standard uncertainty of the measurement of angle α results from the uncertainty propagation rules for indirect measurements, and is given by the following dependence:

$$u(\alpha) = \sqrt{\left(\frac{\partial\alpha}{\partial k}\right)^2\cdot u(k)^2 + \left(\frac{\partial\alpha}{\partial k'}\right)^2\cdot u(k')^2 + \left(\frac{\partial\alpha}{\partial\beta}\right)^2\cdot u(\beta)^2} \quad (27)$$

For the considered measurement stand and the assumed value of angle α, the dependence (27) is shown in graphic form in Fig. 8.

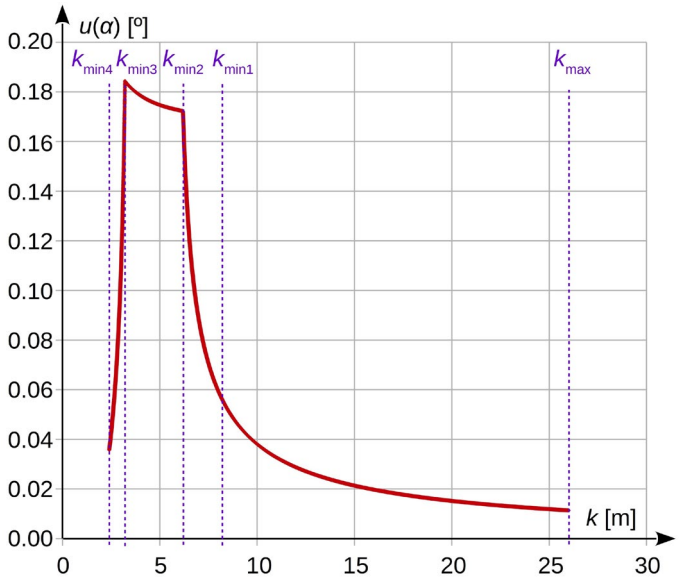

Fig. 8. Dependence of standard uncertainty of angle α measurement in the function of change of distance k

4.3.5. Measurement of the object image position on the surface of matrix x' and y'

The uncertainty of the measurement of the object image position on the surface of an imaging camera matrix results from the stochastic scattering of measurement results for a stationary measurement stand. The said scattering is the result of the impact of accidental factors, such as micro-shocks of the substrate, changes in the lighting levels, temperature changes, etc. Assuming that the measurement time in the considered case is relatively short (from a few to about a dozen seconds), it can be assumed that the parameters such as lighting level or temperature are constant during this period of time. In contrast, the impact of the micro-shock of the substrate on the measurement result will be strictly dependent on distance *k*. In order to determine this dependence, a series of measurements was performed at a stationary measurement stand for the changing distance *k* and the maintained constant reproduction ratio. For each distance a series of 10000 measurements was made, for which the values of standard deviation in the horizontal and vertical axis were determined. These values are the measure of standard uncertainty of measurement of the image position on matrix *x'* and *y'*. The results obtained from the measurements are presented in graphic form in Fig. 9.

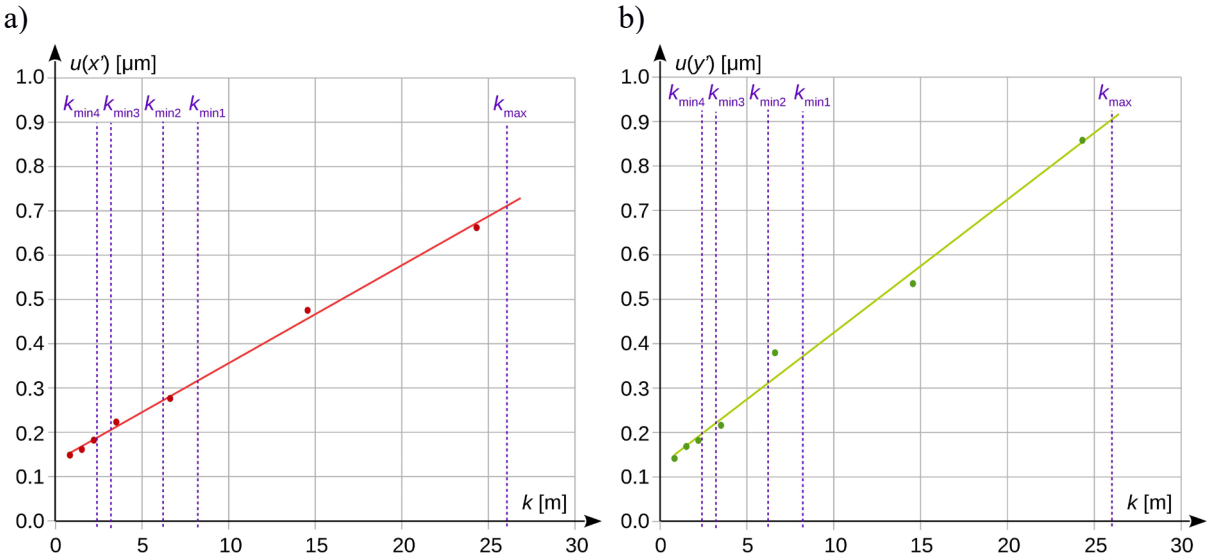

Fig. 9. Standard uncertainties of the measurement of the object image position on the camera matrix, where: a) measurement in horizontal axis; b) measurement in vertical axis

The function expressing the dependence of the uncertainty of the position measurement in the horizontal axis, determined on the basis of linear regression takes the following form (the result in [µm] for *k* expressed in [m]):

$$u(x') = (0.02211 \pm 0.00054) \cdot k + (0.135 \pm 0.006) \quad (28)$$

The analogous dependence for the measurement in vertical axis is given by the following formula:

$$u(y') = (0.0300 \pm 0.0014) \cdot k + (0.125 \pm 0.015) \quad (29)$$

In the case of the considered measurement problem, apart from micro-shocks of the substrate, vibrations caused by the passing vehicle can be expected. The magnitude and degree of the impact of these vibrations depend on numerous factors, whose direct impact is difficult to determine. These will be: the type of ground at the measurement site, the technical condition of the track base, the track, as well as of the passing rolling stock and its driving speed, the way of mounting the camera, including the lens, etc. Due to the nature of displacements of the

contact wire of the overhead contact line caused by the moving current collector, the influence of traffic vibrations on the measurement result can be greatly reduced by filtering the measurement signal. Research shows that frequency of the overhead contact line oscillation amounts to approximately 0.7–1 Hz [1,2], whereas the substrate vibration frequency caused by the rolling stock usually ranges from 30 to 70 Hz [20–24]. By using a low-pass filter, the influence of traffic vibrations on the quality of the measured signal from the imaging camera can be effectively reduced. Sample result of limiting the influence of external vibrations on the measurement is shown in Fig. 10. The vibrations were artificially induced in laboratory conditions. The vibration velocity was measured by attaching the matrix to the imaging camera restraint point. The courses containing the measurement results were subjected to low-pass filtering, with the filter limit frequency of f_{g1} = 11.85 Hz, or f_{g2} = 6.38 Hz.

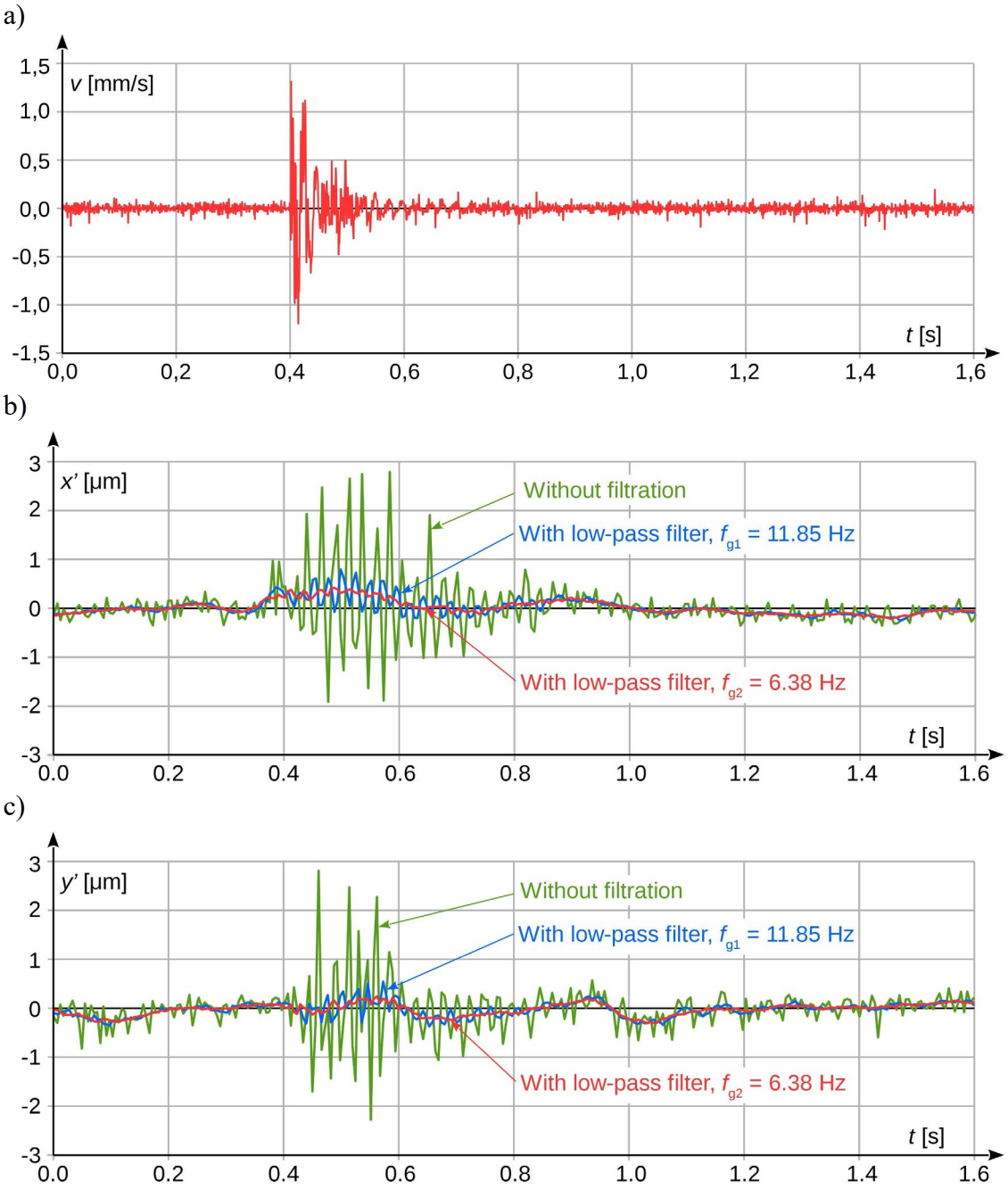

Fig. 10. Limitation of the impact of traffic vibrations on measurement results, where: a) vibration velocity course recorded at the camera mounting point; b) results of measuring the

object image position on the camera matrix in the horizontal axis *x'*; c) results of measuring the object image position on the camera matrix in the vertical axis *y'*

As shown in Fig. 10, the impact of traffic vibrations on measurement results can be effectively reduced by low-pass filtering. However, since such impact cannot be completely eliminated, and taking into consideration the influence of other factors on the camera, which are difficult to define (this requires detailed research), it was assumed that the partial measurement uncertainty associated with determining the position of the object measured on the camera matrix, obtained from the measurements (Fig. 9) will be increased by the factor $k_p = 3$. Such enlarged values will then be adopted as standard uncertainty in measurement of the object image position on the camera matrix.

4.4. Final measurement uncertainty

Taking into account the uncertainty of partial measurements presented in p. 4.3., standard measurement uncertainties of the displacement of the contact wire, obtained from dependencies (6) and (7) in accordance with the propagation uncertainty rules are shown in Fig. 11.

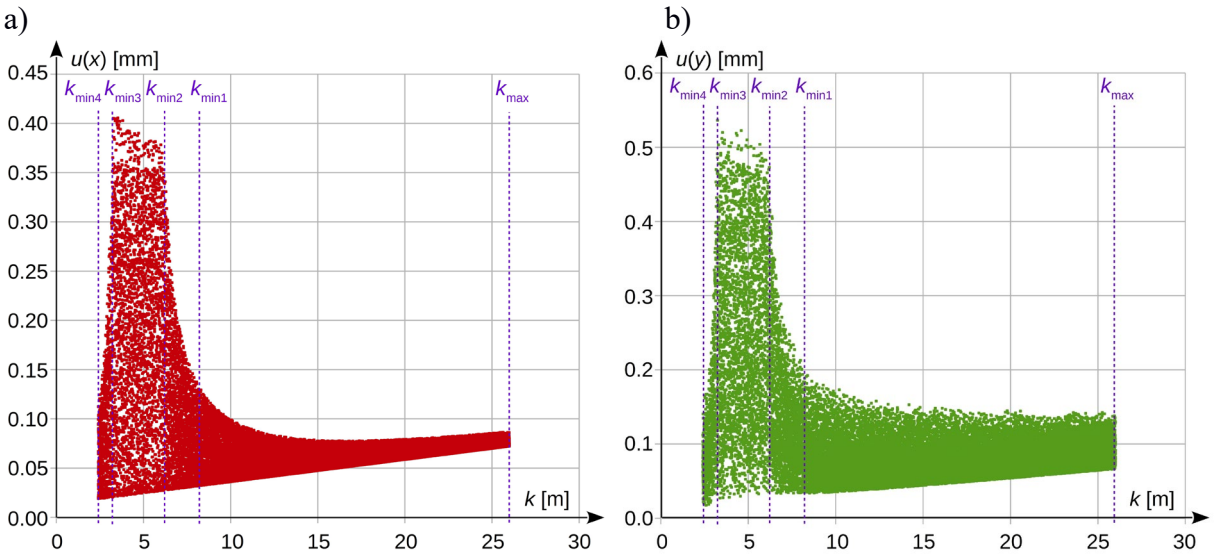

Fig. 11. Standard uncertainties in measurements of the displacement of the contact wire in the function of the distance *k*, where: a) for the measurements in the horizontal axis $u(x)$; b) for the measurements in the vertical axis $u(y)$.

As shown in Figures 11a and b, the maximum value of measurement uncertainty depends on the distance from the measured object. In the case of measurements in the horizontal axis, the minimum for distance $k \approx 16$ m is visible. At a shorter distance, the maximum value of uncertainty rapidly increases, and reaches its highest level range between the distances k_{min2} and k_{min3}. For a distance shorter than k_{min3} the uncertainty is reduced, which is related to the decrease, within this range, of the angle β value and its influence on the measurement uncertainty. For distances *k* longer than 16 m, the value of uncertainty increases slightly, but even for k_{max} it is significantly smaller than the level achieved for k_{min3}.
For measurements in the vertical axis the obtained results are similar to those for the horizontal axis. The difference is that within the considered range of distance *k*, the minimum does not occur and the best results are obtained for distance k_{max}. Additional calculations

show that the smallest uncertainty values occur just for $k \approx k_{max}$, i.e. within the range limit of distance change.
Since the measurements are performed simultaneously in both axes, the distance k between 15 and 20 m is the optimum from the point of view of measurement uncertainty. If the measurement from such a distance is not possible, it will be more advantageous to increase rather than decrease it;. However, it should be pointed out that, within the whole range of the considered changes in distance k, the measurement uncertainties remain at a low level, which is entirely acceptable with regard to the quality of the obtained results.

5. Experimental verification

In order to verify the above considerations, measurements were performed at a laboratory stand. They consisted in the displacement of the contact wire in a vertical and horizontal axis by a known displacement value. Measurements in the vertical axis were performed by analysing physical displacement of the contact wire, but in the horizontal axis, due to the difficulty in realisation of the mechanical construction, the displacement of the contact wire was simulated by measuring the distance between two stationary points, as shown in Fig. 12.

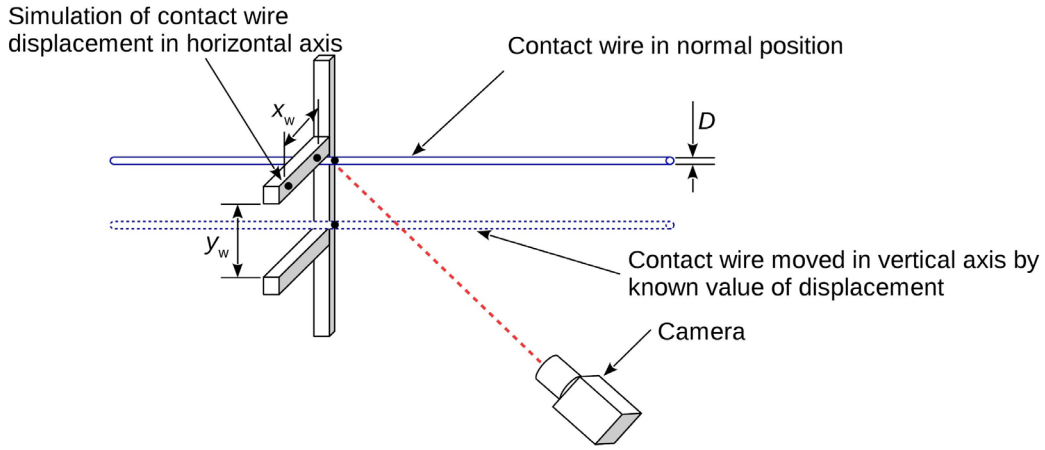

Fig. 12. Verification stand for measurements of contact wire displacement

Measurements were performed for the following output data (standard uncertainty was given for all the parameters):

- distance k = 14549.46 ± 0.87 mm;
- distance F = 582.43 ± 0.23 mm;
- angle α = 42.7200 ± 0.0057º;
- angle β = 5.290 ± 0.067º.

Values y_w and the diameter of the contact wire D were measured using a Yato YT-7201 digital calliper with calibration uncertainty of 0.02 mm for the measurements below 100 mm and 0.03 mm for longer distances. Both measurements were performed ten times, with the following results:

- distance y_w = 109.460 ± 0.018 mm;
- diameter D = 12.215 ± 0.014 mm.

Since the reference value of the contact wire displacement is given by the dependence:

$$y_{pw} = y_w - D \quad (30)$$

given the predetermined values, the obtained reference displacement value with the uncertainty extended for the expansion coefficient $k_p = 2$ was equal to:

$$y_{pw} = 97.245 \pm 0.046 \text{ mm}$$

Afterwards, 14 series of measurements of contact wire displacements were performed, with the use of a vision system. In each series 500 measurements with the wire in the upper position and 500 with the wire in the bottom position were performed. After averaging and calculating the difference, the displacement value was obtained for each series. The results of the sample measurement series are shown in Fig. 13.

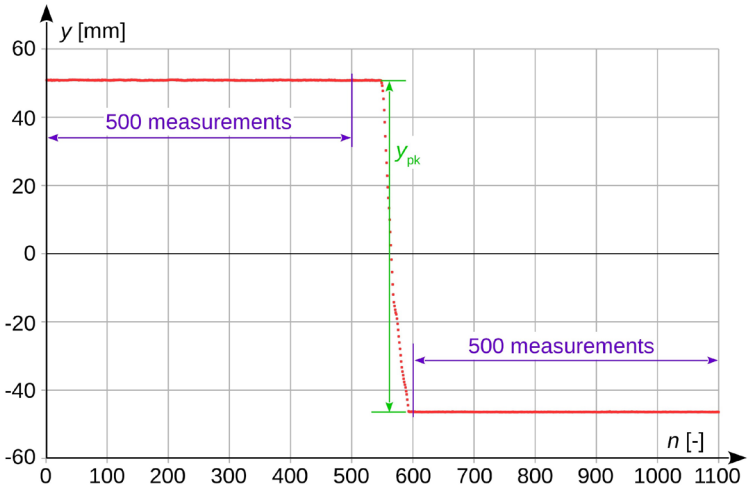

Fig. 13. Results of sample displacement measurement series, where: n – number of measurements

After averaging the obtained results, and determining the uncertainty of types A and B, the displacement value with the extended uncertainty of $k_p = 2$ was obtained, equal to:

$$y_{pk} = 97.21 \pm 0.14 \text{ mm}$$

Analogous measurements for simulation of contact wire displacement in the horizontal axis were performed. For series of reference measurements performed by using a calliper, the result is as follows:

$$x_{pw} = 98.418 \pm 0.042 \text{ mm}$$

Whereas a series of measurements performed by using the vision system resulted in:

$$x_{pk} = 98.47 \pm 0.17 \text{ mm}$$

In both cases the results were given with extended measurement uncertainty for the expansion coefficient $k_p = 2$.

As it can be seen, the difference between the results obtained on the basis of reference measurement and with the use of the vision system fall within the range of measurement uncertainty, for measurements performed in both vertical and horizontal axes. On this basis it

can be stated that the theoretical considerations presented above were confirmed by experimental verification in laboratory conditions.

6. Summary and conclusions

The uncertainty analysis for visual measurement presented in this paper shows that, with regard to the obtained uncertainty, it is reasonable to increase the distance from which the measurements are made. In the discussed case, the optimum results were obtained when the measurements were performed from the distance of several metres. However, for other configurations of the stand or for different measurement ranges, the indicated optimum may be different. The conclusions from the theoretical analysis were confirmed experimentally by performing a series of measurements at the laboratory stand.

The conducted study shows how important it is to perform a measurement uncertainty analysis for a particular test stand. It is particularly significant in visual measurement techniques, as the obtained conclusions may differ from the initial assumptions, the so-called common sense ones. For the stand in question, it would seem that, in order to obtain the greatest accuracy it is reasonable to be as close as possible to the object whose displacement is to be measured. The uncertainty analysis has shown that it is not true, since in the case of a short distance there is a rapid increase in the measurement uncertainty, and better results are achieved when measurements are performed from the distance of a dozen or even more than twenty metres.

During the considerations, the influence of external and internal factors on the uncertainty of the imaging camera itself was treated in a simplified way. Only the impact of increasing distance on the uncertainty of the device was investigated in detail. Therefore, further work will be focused on identifying and investigating the factors which may be relevant to the quality of the measurement signal derived from the analysis of the camera image. It is also planned to use the measurement method in practice, during laboratory and field tests.

Before conducting the research on a real object, it will be necessary to determine the criteria for evaluating the technical condition of the current collector and its contact strip, on the basis of the obtained measurement results of contact wire displacements. Some research on this subject has already been done, but it concerned the results of displacement only in the vertical axis, which had been obtained with the use of another measurement method [2]. Detecting damaged current collector strips on the basis of horizontal contact wire displacements requires elaboration of new diagnostic criteria, which will also constitute the subject of further research.

[1] Vázquez C.A.L., Quintas M.M., Romera M.M., 2010. Non-contact sensor for monitoring catenary-pantograph interaction, in: 2010 IEEE International Symposium on Industrial Electronics. Presented at the 2010 IEEE International Symposium on Industrial Electronics, pp. 482–487. doi:10.1109/ISIE.2010.5637852

[2] Karwowski K., Mizan M., Karkosiński D., 2016. Monitoring of current collectors on the railway line. Transport 0, 1–9. doi:10.3846/16484142.2016.1144222

[3] Skibicki J., 2016. Measurement methods of the overhead traction contact line vibrations. Przegląd Elektrotechniczny R. 92 7/2016, pp. 144–148. doi:10.15199/48.2016.07.32

[4] Galiulin Rav.M., GAliulin Rish.M., Bakirov J.M., Bydanov V.V., Bogdanov D.R., 2000. Optoelectronic measurement of a contact net geometric parameters in railways. IFAC Proceedings Volumes, Volume 33, Issue 20, July 2000, pp. 143–147. doi:10.1016/S1474-6670(17)38040-0

[5] Hofler H., Dambacher M., Dimopoulos N., Jetter V., 2004. Monitoring and inspecting overhead wires and supporting structures, in 2004 IEEE Intelligent Vehicles Symposium/Parma, pp. 512–517. doi:10.1109/IVS.2004.1336436
[6] Cho, C.J., Ko, H., 2015. Video-Based Dynamic Stagger Measurement of Railway Overhead Power Lines Using Rotation-Invariant Feature Matching. IEEE Trans. Intell. Transp. Syst. 16, 1294–1304. doi:10.1109/TITS.2014.2361647
[7] Cho, C.J., Park, Y., 2016. New Monitoring Technologies for Overhead Contact Line at 400 km·h−1. Engineering 2, 360–365. doi:10.1016/J.ENG.2016.03.016
[8] Li F., Li Z., Li Q., Wang D., 2010. Calibration of three CCD camera overhead contact line measuring system, in 2010 International Conference on Intelligent Computation Technology and Automation (ICICTA), Changsha, China, pp. 911–913. doi:10.1109/ICICTA.2010.17
[9] Kusumi S., Nezu K., Nagasawa H., 2000. Overhead Contact Line Inspection System by Rail-and-Road Car. RTRI Vol. 41 (2000) No. 4, pp. 169– 72. doi:10.2219/rtriqr.41.169
[10] Skibicki J., 2013. The new version of contact-less method for localisation of catenary contact wire – theoretical assumption. Przegląd Elektrotechniczny 07/2013 pp. 100–104.
[11] Skibicki J., Bartłomiejczyk M., 2017. Analysis of measurement uncertainty for contact-less method used to measure the position of catenary contact wire, performed with the use of Monte Carlo method. Measurement 97, 203–217. doi:10.1016/j.measurement.2016.11.008
[12] Liu Z., Liu W., Han Z., 2017. A High-Precision Detection Approach for Catenary Geometry Parameters of Electrical Railway. IEEE Trans. Instrum. Meas. pp. 1–11. doi:10.1109/TIM.2017.2666358
[13] Borromeo S., Aparicio J.L., 2002. Automatic system for wear measurement of contact wire in railways, in: 28th Annual Conference of the Industrial Electronic Society, IEEE/Sevilla 2002, pp. 2700–2705. doi:10.1109/IECON.2002.1182821
[14] Shing A.W.C., Pascoschi G., 2006. Contact wire wear measurement and data management, in: IET International Conference on Railway Condition Monitoring, 2006, pp. 182–187. doi:10.1049/ic:20060066
[15] Judek S., Jarzebowicz L., 2014. Algorithm for Automatic Wear Estimation of Railway Contact Strips Based on 3D Scanning Results, in: 2014 International Conference and Exposition on Electrical and Power Engineering (EPE 2014), Iasi, Romania, pp. 724–729. doi:10.1109/ICEPE.2014.6970004
[16] Judek S., Jarzebowicz L., 2015. Wavelet Transform-Based Approach to Defect Identification in Railway Carbon Contact Strips. Elektronika ir Elektrotechnika, Vol 21, No 6 (2015), pp. 29–33. doi:10.5755/j01.eee.21.6.13755
[17] Stefano, E.D., Ruffaldi, E., Avizzano, C.A., 2016. Automatic 2D-3D vision based assessment of the attitude of a train pantograph, in: 2016 IEEE International Smart Cities Conference (ISC2). Presented at the 2016 IEEE International Smart Cities Conference (ISC2), pp. 1–5. doi:10.1109/ISC2.2016.7580747
[18] Jarzebowicz L., Judek S., 2014. 3D machine vision system for inspection on contact strips in railway vehicle current collectors. In: 2014 International Conference on Applied Electronics (AE), Pilsen, Czech Republic. doi:10.1109/AE.2014.7011686
[19] Aydin, I., Karaköse, M., Akin, E., 2013. A Robust Anomaly Detection in Pantograph-Catenary System Based on Mean-Shift Tracking and Foreground Detection, in: 2013 IEEE International Conference on Systems, Man, and Cybernetics. Presented at the 2013 IEEE International Conference on Systems, Man, and Cybernetics, pp. 4444–4449. doi:10.1109/SMC.2013.757
[20] Garinei A., Risitano G., Scappaticci L., Castellani F., 2016. An optimized method to evaluate the performance of trench isolation for railway-induced vibration. Measurement 94, 92–102. doi:10.1016/j.measurement.2016.07.079

[21] Gnyp K., 2014. Wpływ przejeżdżających pociągów w sąsiedztwie projektowanego obiektu na obiekt oraz na przebywających w nim ludzi i urządzenia techniczne. Budownictwo i Architektura 13 1/2014, pp. 29–40
[22] Korzeb J., 2011. Analiza drgań komunikacyjnych z zastosowaniem teorii falek. Prace Naukowe Politechniki Warszawskiej. Transport z. 77/2011, pp. 45–57
[23] Nader M., Purta E., 2011. Oddziaływanie autobusów komunikacji miejskiej na ludzi w otoczeniu dalszym. Logistyka 4/2011, pp. 698–705
[24] Galvin P., Dominguez J., 2009. Experimental and numerical analyses of vibrations induced by high-speed trains on the Cordoba-Malaga line. Soil Dynamics and Earthquake Engineering 29, 641–657. doi:10.1016/j.soildyn.2008.07.001